Journal of Innovative Technology, Vol. 4, No. 2, pp. 53-64, September 2022
http://doi.org/10.29424/JIT.202209_4(2).0006

Seismic Retrofit of Coupled Hospitals with Viscous Dampers

Wang-Chuen Lin[1], Chung-Han Yu[1], Cho-Yen Yang[1], Jenn-Shin Hwang[2,3], Shiang-Jung Wang[4,3 *]

ABSTRACT

When seismically retrofitting existing hospitals, in addition to achieving the desired structural seismic performance, there are certain special requirements that should be taken into consideration, such as accommodating the original structural configuration and space, minimizing the impact on daily operation and patients during the reconstruction period, and guaranteeing the functionality of housed critical medical equipment. A seismic retrofit strategy is thus proposed that involves external connections via linear viscous dampers that have efficiently distributed damping coefficients. Two installation approaches are examined and discussed: damper connections for each story and damper connections for just the lower stories. Three damping coefficient distribution methods are discussed and examined: uniform distribution across all stories, a distribution based on the kinetic energy of all stories, and a more efficient distribution based on the kinetic energy of critical stories. The numerical results show that improper design of the installed reaction structures and linked viscous dampers can be precluded by eliminating those that fall within undesired frequency ratio bands. The three distribution methods are shown to be able to satisfactorily control the seismic response of existing hospitals, and the third distribution method based on the kinetic energy of the critical stories is shown to be the most cost-effective.

Keywords: Seismic retrofit; external connection; viscous damper; viscous damping coefficient; distribution method.

1. INTRODUCTION

During and after the 1999 Chi-Chi earthquake, the operation of numerous otherwise completely intact facilities in Taiwan was interrupted due to moderate to severe structural damage and the malfunction of their non-structural components; this was notably so for hospitals that needed to give medical treatment to individuals who were sick or wounded (Nagarajaiah & Xiaohong, 2000; Alesch, Arendt & Petak, 2005). These damaged or non-functional hospitals could not provide urgent medical treatment to their patients and their inpatients needed to be sent to other medical centers, further hindering the emergency response to the earthquake. As a result, it was recognized that during and after natural disasters such as earthquakes, hospitals play a critical role as they are expected to be responsible for not only the basic safety of patients and staff but also more general disaster relief (Hamburger, 2003; Bachman *et al*., 2003).

Using traditional construction methods for the seismic retrofitting of hospitals often generates significant noise, dust, and vibration, which interfere with everyday operations. Furthermore, due to the numerous independent piping systems running throughout these facilities, the space for the additional openings required for seismic retrofitting can be very limited. These problems exist because seismic retrofitting of school buildings can be carried out during summer or winter vacation, while hospitals are open year-round. Therefore, any chosen construction period disrupts their operations.

Thus, adopting passive control methods may be a more effective and reliable retrofit strategy to strengthen their earthquake-resistant capacities and lower their seismic demands because it would not only increase the performance of existing hospitals during and after earthquakes but also reduce the impact on their daily activities during the seismic retrofit reconstruction process.

When evaluating different strategies for the seismic retrofitting of existing hospitals, there are other major concerns in addition to the structure achieving the desired seismic performance, *e.g*., accommodating the original structural configuration and space, minimizing the impact on daily operations and patients during the reconstruction period, and guaranteeing the functionality of critical medical equipment (or quick restoration after a major earthquake at minimum). In order to meet the above requirements, this study proposes a practical seismic retrofit strategy. Install externally connected viscous dampers as between the existing hospital structure and one or more newly constructed reactive structures. Fig. 1 shows the proposed strategy, where Structure A is the hospital structure to be retrofitted and Structure B is the reactive structure. Figs. 1(a) and 1(b) depict two possible approaches: the first involves connecting viscous dampers to each story and the second involves connecting them to just the lower floors of the existing hospital structure. Conceptually, the proposed seismic retrofit strategy shown in Fig. 1 is like the connection of two adjacent structures by velocity-dependent dampers that have been discussed in many previous studies as a way to simultaneously reduce their wind- or earthquake-induced responses and the likelihood of collision (Maison & Kasai, 1992; Xu, He & Ko, 1999; Zhang &

Manuscript received March 4, 2022; revised March 29, 2022; accepted June 22, 2022.

[1] Associate Researcher, Structural Monitoring and Control Division, National Center for Research on Earthquake Engineering, National Applied Research Laboratories, Taipei, Taiwan.

[2] Professor, Department of Civil and Construction Engineering, National Taiwan University of Science and Technology, Taipei, Taiwan.

[3] Courtesy Researcher, National Center for Research on Earthquake Engineering, National Applied Research Laboratories, Taipei, Taiwan.

[4*] Professor (corresponding author), Department of Civil and Construction Engineering, National Taiwan University of Science and Technology, Taipei, Taiwan. (sjwang@mail.ntust.edu.tw)

Xu, 1999, 2000; Matsagar & Jangid, 2005; Bhaskararao & Jangid, 2007; Hwang *et al.* 2007).

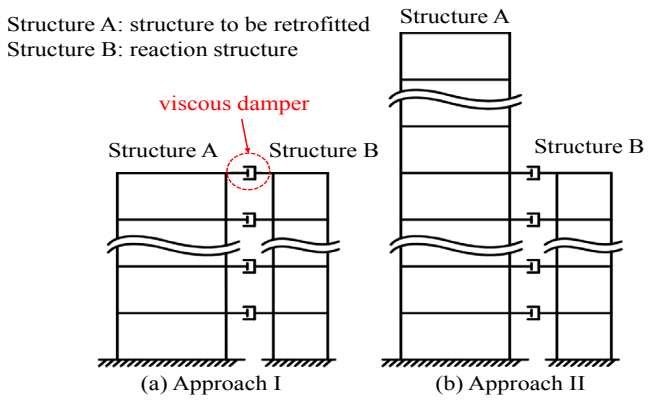

Fig. 1 Proposed seismic retrofit strategy: external connections of viscous dampers to (a) all stories and (b) only the lower stories.

When two adjacent structures linked by viscous dampers have the same primary modal period, any phase angle between their movements could be induced by the first mode shapes, resulting in entirely different control performances for the linked dampers. With a phase angle of 0°, the connected dampers have no relative displacement and do not work, whereas with a phase angle of 180° the linked dampers have the most significant relative displacement and thus perform most efficiently. Hwang *et al.* (2007) established a relationship between the phase lag of two adjacent single-degree-of-freedom (SDOF) systems and the actual effect of the connected damper. It was analytically verified that there is a correlation between the natural frequency ratio of the two systems and the added damping ratio. Therefore, a concept for preventing the frequency ratio of the two adjacent structures from falling into the undesired band was proposed to ensure that the linked dampers enhanced the damping ratios of the two structures.

In addition to design formulas used to estimate the increase of the damping ratio of the buildings (FEMA 273, 1997; Seleemah & Constantinou, 1997; FEMA 356, 2000; Hwang *et al.* 2008), some studies have further discussed the optimal design of viscous dampers for new construction and retrofit purposes in terms of their placement and the vertical distribution of their damping coefficients (Singh & Moreschi, 2002; Wongprasert & Symans, 2004; Takewaki, 2005; Hwang, Lin & Wu, 2013; Lin, Hwang & Chen, 2017). Hwang *et al.* (2013) proposed two non-repetitive design formulas to vertically distribute the damping coefficients of viscous dampers to achieve a desired additional damping ratio, which was based on the ratio of the strain energy of a story to the total shear strain energy of the structure. The numerical results indicated that the distribution method based on the shear strain energy of a story was the more practical and efficient option. With respect to the same structural model, Lin *et al.* (2017) further employed two search methods based on genetic algorithms to investigate the optimal distribution of the damping coefficients of viscous dampers. The comparison showed that, although these different methods produced a comparable seismic response reduction for the same supplemental damping ratio, the method proposed by Hwang *et al.* (2013) generally performed better.

This study proposes a seismic retrofitting method that involves the installation of linear viscous dampers to connect an existing hospital structure to a newly built reaction structure, as presented in Fig. 1. The undesired frequency ratio band of the two multi-degree-of-freedom (MDOF) structures is the first identified using only their fundamental modal characteristics. Then, two distribution methods for the damping coefficients of the externally connected dampers are derived on the basis of the ratio of the relative kinetic energy at each story to the total relative kinetic energy of the entire hospital structure. Several instances are numerically examined and compared with the counterparts derived using traditional uniform distribution methods.

2. TWO SDOF SYSTEMS LINKED BY A VISCOUS DAMPER

2.1 RELEVANT THEORIES AND ASSUMPTIONS

Hospital structures in Taiwan are usually low- or medium-rise buildings. Therefore, their dynamic behavior can be reasonably approximated by the fundamental translational modal characteristics and responses; in other words, the MDOF system can be simplified as an SDOF system. Firstly, the effective modal mass of the MDOF system should be calculated using the following equation:

$$M^* = \frac{\left(\sum_i m_i \phi_i\right)^2}{\sum_i m_i \phi_i^2} \tag{2.1}$$

where M^* is the fundamental modal mass of the MDOF system, m_i is the mass assigned to the i^{th} story, and ϕ_i is the normalized mode shape of the first mode at the i^{th} story ($\phi_{roof} = 1$).

Two SDOF systems connected by a viscous damper are presented in Fig. 2, in which M^*, c, and k are the effective modal mass, damping coefficient, and stiffness of the structure, respectively. The variable subscripts denote which structure it belongs to; a refers to Structure A *(i.e.*, the hospital to be retrofitted) and b refers to Structure B (the reaction structure). c_d is the damping coefficient of the linked viscous damper.

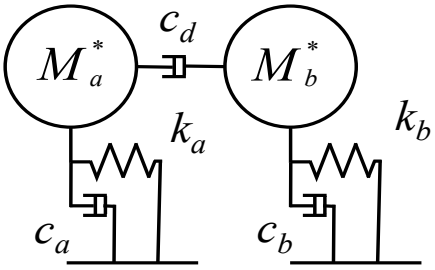

Fig. 2 Schematic illustration of two SDOF systems connected by a viscous damper.

After installing a linear viscous damper, the equation of motion of the resulting system presented in Fig. 2 can be written in matrix form as:

$$[m]\{\ddot{x}\} + [c]\{\dot{x}\} + [k]\{x\} = -[m]\{1\}\ddot{x}_g \tag{2.2}$$

$$\text{where } [m]=\begin{bmatrix} M_a^* & 0 \\ 0 & M_b^* \end{bmatrix};$$

$$[c]=\begin{bmatrix} c_a+c_d & -c_d \\ -c_d & c_b+c_d \end{bmatrix};\ [k]=\begin{bmatrix} k_a & 0 \\ 0 & k_b \end{bmatrix};$$

$$\{x\}=\begin{Bmatrix} x_a \\ x_b \end{Bmatrix};\ \{\dot{x}\}=\begin{Bmatrix} \dot{x}_a \\ \dot{x}_b \end{Bmatrix};\{\ddot{x}\}=\begin{Bmatrix} \ddot{x}_a \\ \ddot{x}_b \end{Bmatrix};$$

and x_a, $\dot{x}_a$, and $\ddot{x}_a$ are the horizontal displacement, velocity, and acceleration of Structure A relative to the ground, respectively, x_b, x_b, and $\ddot{x}_b$ are the horizontal displacement, velocity, and acceleration of Structure B relative to the ground, respectively, and $\ddot{x}_g$ is the input ground acceleration.

Based on the proportional damping assumption, the effective damping ratios of Structures A and B (denoted as $\xi_{eff,a}$ and $\xi_{eff,b}$, respectively) are calculated from:

$$\xi_{eff,a}=\frac{c_a+c_d}{2M_a^*\omega_a}=\xi_a+\frac{c_d}{2M_a^*\omega_a}=\xi_a\left(1+\frac{c_d}{c_a}\right) \text{ and} \quad (2.3.1)$$

$$\xi_{eff,b}=\frac{c_b+c_d}{2M_b^*\omega_b}=\xi_b+\frac{c_d}{2M_b^*\omega_b}=\xi_b\left(1+\frac{c_d}{c_b}\right), \quad (2.3.2)$$

where $\omega_a=(k_a/M^*_a)^{0.5}$, $\omega_b=(k_b/M^*_b)^{0.5}$, $\xi_a=c_a/(2M^*_a\omega_a)$, and $\xi_b=c_b/(2M^*_b\omega_b)$.

Based on the non-proportional damping assumption, the motion equation can be expressed as:

$$\{\dot{z}\}=[A]\{z\}+\{E\}\ddot{x}_g, \quad (2.4)$$

$$\text{where } \{z\}=\begin{Bmatrix} \{x\} \\ \{\dot{x}\} \end{Bmatrix};\ \{\dot{z}\}=\begin{Bmatrix} \{\dot{x}\} \\ \{\ddot{x}\} \end{Bmatrix};$$

$$[A]=\begin{bmatrix} [0] & [I] \\ -[m]^{-1}[k] & -[m]^{-1}[c] \end{bmatrix};$$

$$\text{and } \{E\}=\begin{Bmatrix} \{0\} \\ -\{1\} \end{Bmatrix}.$$

By solving the eigenvalue problem, it can be obtained:

$$\left|([A]-\lambda[I])\right|=\begin{vmatrix} -\lambda & 0 & 1 & 0 \\ 0 & -\lambda & 0 & 1 \\ -\frac{k_a}{M_a^*} & 0 & -\frac{(c_a+c_d)}{M_a^*}-\lambda & \frac{c_d}{M_a^*} \\ 0 & -\frac{k_b}{M_b^*} & \frac{c_d}{M_b^*} & -\frac{(c_b+c_d)}{M_b^*}-\lambda \end{vmatrix}=0 \quad (2.5)$$

By defining $c_a/M^*_a=2\xi_a\omega_a$, $c_b/M^*_b=2\xi_b\omega_b$, and $\lambda=\omega_a R$, Eq. (2.5) can be rewritten as:

$$\begin{aligned} &R^4+\left[2\xi_b\left(\frac{\omega_b}{\omega_a}\right)\left(1+\frac{c_d}{c_b}\right)+2\xi_a\left(1+\frac{c_d}{c_a}\right)\right]R^3 \\ &+\left[4\xi_a\xi_b\left(\frac{\omega_b}{\omega_a}\right)\left(1+\frac{c_d}{c_a}+\frac{c_d}{c_b}\right)+1+\left(\frac{\omega_b}{\omega_a}\right)^2\right]R^2 \\ &+\left[2\xi_a\left(\frac{\omega_b}{\omega_a}\right)^2\left(1+\frac{c_d}{c_a}\right)+2\xi_b\left(\frac{\omega_b}{\omega_a}\right)\left(1+\frac{c_d}{c_b}\right)\right]R+\left(\frac{\omega_b}{\omega_a}\right)^2=0 \end{aligned}, \quad (2.6)$$

where ω_b/ω_a is the ratio of the fundamental modal angular frequency of Structure B to that of Structure A and c_d/c_a and c_d/c_b are the ratios of the damping coefficient of the connected linear viscous damper to the damping coefficients of Structures A and B, respectively.

The eigenvalue can be solved from Eq. (2.5) in a complex form as:

$$\lambda_n=\alpha_n+i\beta_n \text{ and } \bar{\lambda}_n=\alpha_n-i\beta_n, (n=1, 2), \quad (2.7)$$

where λ_n is the n^{th} modal eigenvalue, $\bar{\lambda}_n$ is the conjugate of λ_n, $\alpha_n=-\xi_n\omega_n$, $\beta_n=\omega_n(1-\xi^n)^{0.5}$, ω_n is the n^{th} modal angular frequency, and ξ_n is the n^{th} modal composite damping ratio. ω_n and ξ_n can be further expressed as:

$$\omega_n=\sqrt{\alpha_n^2+\beta_n^2} \text{ and} \quad (2.8)$$

$$\xi_n=\frac{-\alpha_n}{\sqrt{\alpha_n^2+\beta_n^2}}. \quad (2.9)$$

The eigenvector and the conjugate eigenvector can be obtained from:

$$\begin{Bmatrix} \{\phi_n\} \\ \lambda_n\{\phi_n\} \end{Bmatrix} \text{ and } \begin{Bmatrix} \{\bar{\phi}_n\} \\ \bar{\lambda}_n\{\bar{\phi}_n\} \end{Bmatrix}, \quad (2.10)$$

where $\{\phi_n\}$ is the n^{th} mode shape vector and $\{\bar{\phi}_n\}$ is the conjugate vector of $\{\phi_n\}$.

By considering the correlation between the modal composite damping ratio ξ_n and the phase lag of Structures A and B, the two components of $\{\phi_n\}$, *i.e.*, ϕ_{an} and ϕ_{bn}, can be expressed as:

$$\{\phi_n\}=\begin{Bmatrix} \phi_{an} \\ \phi_{bn} \end{Bmatrix}=\begin{Bmatrix} A_{an}e^{i\theta_{an}} \\ A_{bn}e^{i\theta_{bn}} \end{Bmatrix}, (n=1, 2), \quad (2.11)$$

where A_{an} and A_{bn} are the amplitudes of Structures A and B, respectively and θ_{an} and θ_{bn} are the phase angles of Structures A and B, respectively.

By using $\xi_n=C_n/[2(M_nK_n)^{0.5}]$, in which M_n, C_n, and K_n are respectively the generalized mass, damping, and stiffness matrices, the n^{th} modal composite damping ratio ξ_n can be expressed as:

$$\xi_n=\frac{(c_a+c_d)A_{an}^2+(c_b+c_d)A_{bn}^2-2c_dA_{an}A_{bn}\cos(\theta_{an}-\theta_{bn})}{2\sqrt{(M_a^*A_{an}^2+M_b^*A_{bn}^2)(k_aA_{an}^2+k_bA_{bn}^2)}}. \quad (2.12)$$

By solving Eq. (2.6) and using the relationships given in Eqs. (2.7) and (2.9), together with ξ_a and ξ_b set to 5%, ω_b/ω_a varying from 0.1 to 10, c_d/c_a varying from 1 to 6 with an increment of 1, and c_d/c_b varying from 1 to 12 with an increment of 1, then the variations of the n^{th} modal composite damping ratios ξ_n and the n^{th} modal phase lag of Structures A and B, θ_{an}-θ_{bn}, derived using the different values of ω_b/ω_a, c_d/c_a, and c_d/c_b can be quantitatively calculated and discussed. The calculations of the first and second modal composite damping ratios, ξ_1 and ξ_2, with $c_d/c_a = 5$ are shown in Figs. 3 and 4, respectively. The calculations of the first modal phase lag with $c_d/c_a = 5$ are shown in Fig. 5. Each chart can be divided into anterior, intermediate, and posterior segments with respect to ω_b/ω_a.

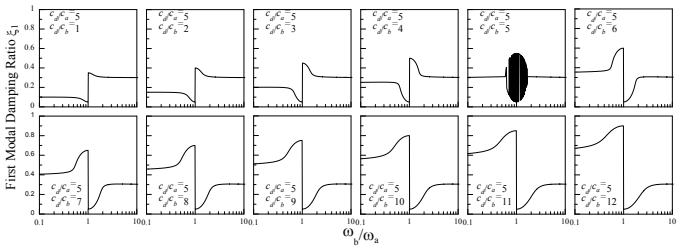

Fig. 3 Variation of ξ_1 for various ω_b/ω_a ($c_d/c_a = 5$, $c_d/c_b = 1$–12).

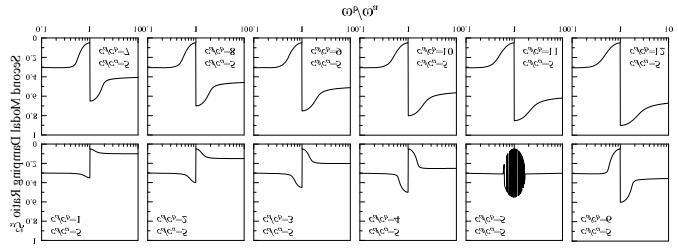

Fig. 4 Variation of ξ_2 for various ω_b/ω_a ($c_d/c_a = 5$, $c_d/c_b = 1$–12).

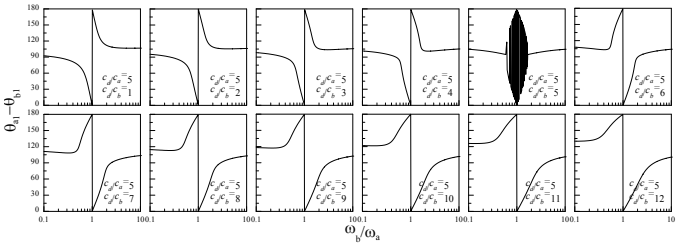

Fig. 5 Variation of (θ_{a1}-θ_{b1}) for various ω_b/ω_a ($c_d/c_a = 5$, $c_d/c_b = 1$–12).

As observed in Figs. 3 and 4, the variation of ξ_1 and ξ_2 for various ω_b/ω_a are skew-symmetric with respect to $\omega_b/\omega_a = 1$. When ω_b/ω_a is closer to one (*i.e.*, in the intermediate segment), ξ_1 and ξ_2 have a more sensitive and unstable variation with ω_b/ω_a. As ω_b/ω_a moves away from one (*i.e.*, in the anterior or posterior segment), ξ_1 and ξ_2 stabilize *(i.e.*, they approach $\xi_{eff,a}$ or $\xi_{eff,b}$ in the anterior or posterior segment). Eq. (2.12) shows that the modal composite damping ratio and phase lag are correlated. As shown in Fig. 5, when ω_b/ω_a is closer to one, the first modal phase lag becomes more unstable, which can further explain the phenomenon showed in Fig. 3. The same trend can be found for the second modal phase lag. To be more precise, the instability of the modal composite damping ratio is caused by the significant variation of the modal phase lag. Based on the non-proportional damping assumption, any phase angle between the motions of Structures A and B caused by their dominant mode shapes can exist as ω_b/ω_a approaches one, especially when c_d/c_a is equal to c_d/c_b. In this case, the analytical results indicate entirely different and unstable control performance, *i.e.*, entirely different and unstable modal composite damping ratios. Therefore, care should be taken to avoid observing unstable frequency-ratio bands (*i.e,* intermediate segments) in practical designs. With given values of ξ_a, ξ_b, c_d/c_a, and c_d/c_b, calculated values of $|\xi_n\text{-}\xi_{eff,a}|/\xi_{eff,a}$ and $|\xi_n\text{-}\xi_{eff,b}|/\xi_{eff,b}$ less than 0.02 are chosen to quantitatively define the lower and upper bounds of the undesired frequency ratio band. The undesired frequency ratio bands with $c_d/c_a = 1$–6 and $c_d/c_b = 1$–12 for $\xi_a = \xi_b = 5\%$ are showed in Fig. 6.

Consequently, when adopting the seismic retrofit strategy proposed, the new structure is designed to obtain the preliminary fundamental modal frequency. After the target damping ratio of the hospital structure is determined, the total damping coefficient of the connected linear viscous dampers can be obtained by Eq. (2.3.1) or (2.3.2). The calculated values of ω_b/ω_a, c_d/c_a, and c_d/c_b must be examined to ensure that they do not fall in the undesired frequency ratio band indicated in Fig. 6. For the design values of ξ_a, ξ_b, c_d/c_a, and c_d/c_b that differ from the values used in Fig. 6, the undesired frequency ratio band can be obtained simply through linear interpolation or be recalculated on a case-by-case basis. Then, the damping coefficient of each damper can be calculated by the uniform distribution concept, as quantitatively demonstrated in subsection 2.2, or else based on one of the more sophisticated concepts introduced in Section 3.

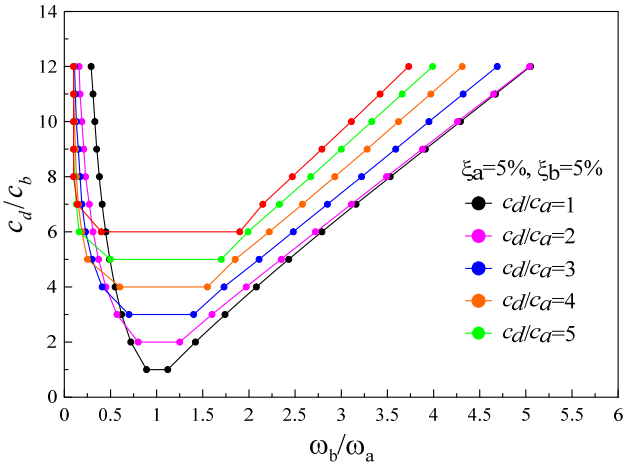

Fig. 6 Undesired frequency ratio bands for $\xi_a = \xi_b = 5\%$ ($c_d/c_a = 1$–6, $c_d/c_b = 1$–12).

2.2 DEMONSTRATION EXAMPLES

As shown in Fig.7, a two-dimensional model consisting of two structures linked by linear viscous dampers was numerically analyzed. Structure A is an existing regular 10-story hospital structure to be retrofitted. The heights of the first and subsequent stories were 4 m and 3.5 m, and the calculated fundamental modal period in the X direction was 1.085 s. Structure B (one span) represents the newly designed reaction structure. Each story height was identical to Structure A, and for Approach I (in which all stories were connected) it was designed as a 10-story structure

but for Approach II (in which the lower stories were connected) it was a 5-story structure. Both structures were assumed to have an inherent damping ratio of 5%, which may be too high empirically for steel structures but was acceptable for the purposes of demonstration.

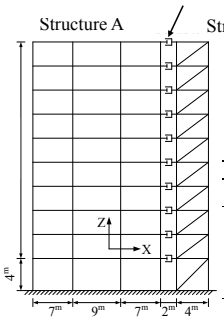

Structure A

Story	Beam (mm)	Column (mm)	Mass (kN·s²/m)
1F and 2F	H 692×400×16×36	700x700x36x36	147.2
3F	H 692×400×16×36	650x650x36x36	147.2
4F and 5F	H 684×400×16×32	650x650x36x36	138.0
6F	H 684×400×16×32	650x650x36x36	119.6
7F to10F	H 592×400×16×36	650x650x32x32	119.6

Structure B

Story	Beam (mm)	Column (mm)	Brace (mm)	Mass (kN·s²/m)
1F	H 400x400x13x21	600x600x36x36	267.4x9.3	5.77
2F	H 400x400x13x21	600x600x36x36	267.4x9.3	5.46
3F	H 400x400x13x21	600x600x36x36	267.4x9.3	4.98
4F and 5F	H 400x400x13x21	600x600x28x28	267.4x9.3	4.5
6F	H 400x400x13x21	600x600x28x28	267.4x9.3	4.14
7F to 9F	H 400x400x13x21	600x600x22x22	267.4x9.3	3.78
10F	H 400x400x13x21	600x600x22x22	267.4x9.3	2.23

(a) Approach I

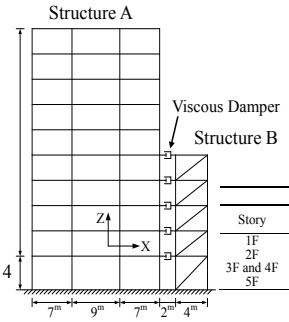

Structure B

Story	Beam (mm)	Column (mm)	Brace (mm)	Mass (kN·s²/m)
1F	H 400×400×13×21	550×550×36×36	267.4×9.3	4.93
2F	H 400×400×13×21	550×550×36×36	267.4×9.3	3.98
3F and 4F	H 400×400×13×21	500×500×22×22	267.4×9.3	3.3
5F	H 400×400×13×21	500×500×22×22	267.4×9.3	1.98

(b) Approach II

Fig. 7 Demonstration examples of the two-dimensional models.

In Approach I, ten linear viscous dampers were installed to connect Structure A with Structure B at all stories, as illustrated in Fig. 7(a). The fundamental modal period of Structure B in the X direction was calculated as 0.179 s when only considering its self-weight, which implies that Structure B played the role of the displacement-controlled structure. The effective modal masses of Structures A and B were $M_a^* = 1017.71$ kN·s^2/m and $M_b^* = 33.15$ kN·s^2/m, respectively. The fundamental modal angular frequencies of Structures A and B were 5.79 rad/s and 35.10 rad/s, respectively. The effective modal damping coefficients of Structures A and B were calculated as $c_a = 2M_a^* \omega_a \xi_a = 589.4$ kN·s/m and $c_b = 2M_b^* \omega_b \xi_b = 116.4$ kN·s/m, respectively. After determining a target damping ratio of 15% for Structure A, the total damping coefficient of the connected linear viscous dampers could then be calculated as $c_d = 2M_a^* \omega_a(\xi_{eff}-\xi_a) = 1178.7$ kN·s/m.

In Approach II, five linear viscous dampers were installed to connect the lower five stories of Structure A with Structure B, as shown in Fig. 7(b). The fundamental modal period of Structure B in the X direction was calculated as 0.082 s, which implies that Structure B played the role of the displacement-controlled structure. The effective modal masses of Structures A and B were $M_a^* = 1017.71$ kN·s^2/m and $M_b^* = 14.68$ kN·s^2/m, respectively. The fundamental modal angular frequencies of Structures A and B were 5.79 rad/s and 76.62 rad/s, respectively. The effective modal damping coefficients of Structures A and B were calculated as $c_a = 2M_a^* \omega_a \xi_a = 589.4$ kN·s/m and $c_b = 2M_b^* \omega_b \xi_b = 112.5$ kN·s/m, respectively. After determining a target damping ratio of 15% for Structure A, the total damping coefficient of the connected linear viscous dampers could then be calculated as $c_d = 2M_a^* \omega_a(\xi_{eff}-\xi_a) = 1178.7$ kN·s/m.

As presented in Fig. 8, by reasonably assuming Structures A and B were represented by two SDOF systems, when the ratio ω_b/ω_a of Approaches I and II were 6.06 and 13.23, respectively, the c_d/c_b of Approaches I and II were 10.13 and 10.48, respectively, and the c_d/c_a of both approaches was 2, the design parameters did not fall in the undesired frequency ratio range. Based on the concept of uniform distribution, the damping coefficient of each damper for Approaches I and II was designed as 117.87 kN·s/m and 235.74 kN·s/m, respectively.

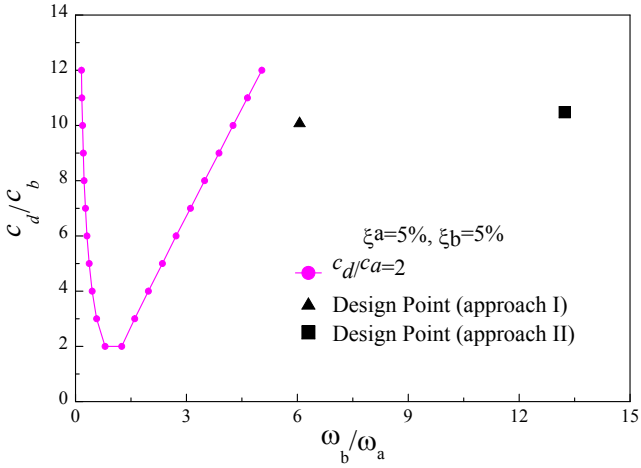

Fig. 8 Undesired frequency ratio bands for the demonstration examples.

Figs. 9(a) and 9(b) illustrate the roof displacement response of Structure A subjected to a ground motion when adopting Approaches I and II, respectively. Each was compared with the response of Structure A with an inherent damping ratio of 15%. It appears that neither retrofit approach could reduce the response as effectively as an inherent damping ratio of 15%. By using the logarithmic decay method, the damping ratios of Structure A when adopting Approaches I and II were calculated as 13.19% and 7.57%, respectively. The values are lower than the target damping ratio of 15%, especially for Approach II. This may be due to the overestimation of the damping effect without adequate consideration of the flexural behavior of Structure A. Furthermore, the rationale behind using the uniform distribution method may require further study. These concerns will be more thoroughly discussed in Section 4.

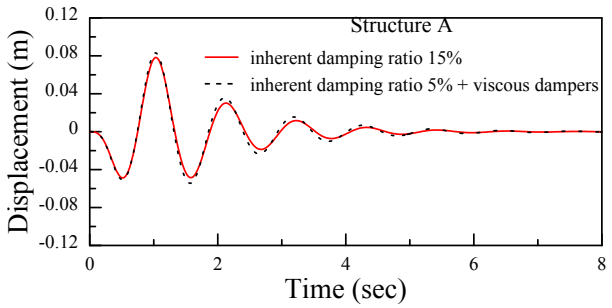

(a) Approach I

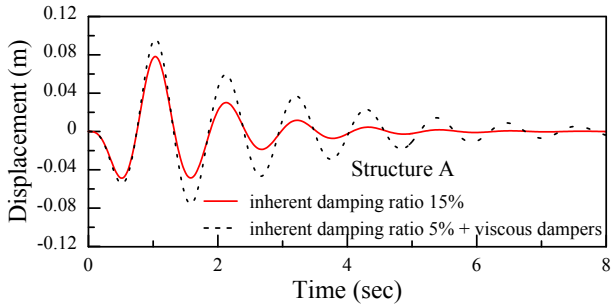

(b) Approach II

Fig. 9 Roof displacement responses of Structure A with a target damping ratio of 15% under a ground acceleration impulse.

3. DISTRIBUTION OF DAMPING COEFFICIENTS BASED ON ENERGY APPROACHES

3.1 RELEVANT THEORIES AND ASSUMPTIONS

Since Approach II involves the linear viscous dampers only being connected to the lower five stories of Structure A, as shown in Fig. 7(b), the dampers directly contribute to their (the lower five stories) energy dissipation. Therefore, evenly distributing the total damping coefficient among these dampers may not be the most appropriate approach. The relationship between the total strain energy of the multi-DOF structure and the energy dissipation of each story of viscous dampers should be considered. Assuming the same mechanical properties and installation of one layer of linear viscous dampers, the supplemental damping ratio provided by all dampers can be calculated (FEMA 273, 1997; FEMA 356, 2000):

$$\xi_d = \frac{T\sum_j c_j \cos^2\theta_j \phi_{rj}^2}{4\pi\sum_i m_i \phi_i^2}, \tag{3.1}$$

where T is the fundamental modal period of the structure, c_j is the damping coefficient of the dampers at the j^{th} story, θ_j is the inclination angle of the dampers at the j^{th} story, ϕ_{rj} is the first modal relative displacement between the two ends of the dampers on the j^{th} story in the horizontal direction, m_i is the mass assigned to the i^{th} story, and ϕ_i is the normalized mode shape of the first mode at the i^{th} story ($\phi_{roof} = 1$).

Overall, the initial modal period of the hospital structure to be retrofitted was much longer than that of the reaction structure; however, during derivation, it was assumed to behave as a rigid body for simplicity because the ϕ_{rj} of the dampers connected to the j^{th} story was identical to ϕ_i. Therefore, Eqs. (2.3.1) and (2.3.2) can be expressed as:

$$\frac{c_d}{2M_a^*\omega_a} = \xi_d = \frac{T_a\sum_r C_r\phi_r^2}{4\pi\sum_N m_N\phi_N^2} \text{ and} \tag{3.2.1}$$

$$\frac{c_d}{2M_b^*\omega_b} = \xi_d = \frac{T_b\sum_r C_r\phi_r^2}{4\pi\sum_N m_N\phi_N^2}, \tag{3.2.2}$$

where T_a and T_b are the fundamental modal periods of Structures A and B, respectively, C_r is the damping coefficient of the dampers connected to the r^{th} story of Structure A, ϕ_r is the first modal relative displacement between the two ends of the dampers on the r^{th} story in the horizontal direction, m_N is the mass assigned to the N^{th} story of Structure A, ϕ_N is the normalized mode shape of the first mode at the N^{th} story of Structure A ($\phi_{roof} = 1$), N is the total number of stories of Structure A, and r is the total number of stories linked by the dampers.

As observed from Eq. (3.2.1) and Eq. (3.2.2), c_d can be obtained by any arbitrary combination of C_r for a given set of structural parameters. With ω_b/ω_a always larger than one, only Eq. (3.2.1) is required to further derive and discuss the following three methods for distributing the damping coefficients among the viscous dampers connecting Structures A and B.

3.2 UNIFORM DISTRIBUTION

The uniform distribution (UD) method equalizes the damping coefficients of viscous dampers at different stories (*i.e.*, $C_r = C$). This method is simple and convenient for engineering practices. By using Eq. (3.2.1), the formula for calculating the damping coefficient of linear viscous dampers at each story can be calculated from:

$$C = \frac{c_d\sum_N m_N\phi_N^2}{M_a^*\sum_r \phi_r^2} = \frac{4\pi\xi_d\sum_N m_N\phi_N^2}{T_a\sum_r \phi_r^2}. \tag{3.3}$$

Because seismic demands on dampers at different stories are not the same in reality, the UD method may not be the most efficient.

3.3 DISTRIBUTION BASED ON STORY KINETIC ENERGY

From Hwang *et al*. (2013) and Lin *et al.* (2017), the distribution method that the damping coefficient of the viscous damper is proportional to the ratio of the floor strain energy to the total shear strain energy of the structure is practical and effective. Compared to installing viscous dampers inside the structure, where the reaction structure behaves as a relatively rigid body, the relative displacement response of the damper connected between the hospital structure to be retrofitted and the reaction structure can simply be assumed to be proportional to the first mode of the hospital. Furthermore, the seismic input energy is theoretically equal to the sum of the kinetic energy, elastic strain, hysteresis and viscous damping energy of the system. Therefore, this distribution method was chosen in this study. This method is hereinafter referred to as the story kinetic energy (SKE) method. This method is more reasonable than the UD method. This is because installing viscous dampers with larger damping coefficients at stories with larger relative kinetic energy has a greater contribution to the system damping ratio.

The damping coefficient of the viscous dampers connected to the r^{th} story of the hospital structure based on the relative kinet-

ic energy at the i^{th} story being proportional to $m_i\phi_i^2$ can be expressed as:

$$C_r = pm_r\phi_r^2, \tag{3.4}$$

where p is a proportionality constant. The total damping coefficient of all viscous dampers can then be obtained from:

$$\sum_r C_r = \sum_r pm_r\phi_r^2 = p\sum_r m_r\phi_r^2 . \tag{3.5}$$

By rearranging Eq. (3.4) to obtain $p = C_r/(m_r\phi_r^2)$ and substitutingit into Eq. (3.5) to obtain $\sum_r C_r = C_r\sum_r m_r\phi_r^2 \Big/ (m_r\phi_r^2)$, and then substituting that into Eq. (3.2.1), the formula to alculate the damping coefficient of linear viscous dampers at the rth story can be obtained as:

$$C_r = \frac{c_d m_r\phi_r{}^2\sum_N m_N\phi_N{}^2}{M_a^*\sum_r m_r\phi_r^4} = \frac{4\pi\xi_d m_r\phi_r{}^2\sum_N m_N\phi_N{}^2}{T_a\sum_r m_r\phi_r^4}. \tag{3.6}$$

3.4 DISTRIBUTION BASED ON STORY KINETIC ENERGY TO EFFICIENT STORIES

To improve the effectiveness of the SKE method, viscous dampers could be installed at appropriate stories where their relative kinetic energies are larger than the average relative kinetic energy, as below.

$$m_i\phi_i^2 > \frac{\sum_i m_i\phi_i^2}{N}. \tag{3.7}$$

With the criterion given in Eq. (3.7) and by substituting Eqs. (3.4) and (3.5) into Eq. (3.2.1), the formula to distribute the total damping coefficients among the linear viscous dampers installed at appropriate stories is:

$$C_r = \frac{c_d m_l\phi_l{}^2\sum_N m_N\phi_N{}^2}{M_a^*\sum_l m_l\phi_l^4} = \frac{4\pi\xi_d m_l\phi_l{}^2\sum_N m_N\phi_N{}^2}{T_a\sum_l m_l\phi_l^4}, \tag{3.8}$$

where l is the number of stories that have relative kinetic energies larger than the average relative kinetic energy. This method is called the story kinetic energy to efficient stories (SKEES) method hereafter.

3.5 DEMONSTRATION EXAMPLES

The same model and retrofit approaches presented in Fig. 7 were used to further compare the control performances using the UD method (as given in Eq. (3.3)), the SKE method (Eq. (3.6)), and the SKEES method (Eq. (3.8)). The distributions of the damping coefficients of the hospital structure calculated as per Eqs. (3.3), (3.6), and (3.8) for Approaches I and II are listed in Table 1.

Table 1 Distribution of the damping coefficients of the 10-story hospital structure for Approaches I and II based on UD, SKE, and SKEES.

Story	Approach I			Approach II		
	UD (kN·s/m)	SKE (kN·s/m)	SKEES (kN·s/m)	UD (kN·s/m)	SKE (kN·s/m)	SKEES (kN·s/m)
10	142.2	194.8	207.6	-	-	-
9	142.2	178.0	189.7	-	-	-
8	142.2	154.4	164.5	-	-	-
7	142.2	125.3	133.6	-	-	-
6	142.2	95.1	101.4	-	-	-
5	142.2	77.1	-	911.2	1253.1	1363.2
4	142.2	47.7	-	911.2	775.8	843.9
3	142.2	26.1	-	911.2	423.5	-
2	142.2	9.4	-	911.2	153.3	-
1	142.2	1.5	-	911.2	25.1	-
Total	1422.0	909.5	796.7	4556.0	2630.8	2207.1

Table 1 states that the total damping coefficient when using the UD method is greater than when using the other methods. For the SKE and SKEES methods, the higher the story, the larger the damping factor assigned to that story. For Approach I, the UD, SKE, and SKEES methods all produce damping ratios close to 14.83%, which is close to the target damping ratio of 15%. For Approach I, the damping ratios calculated using the UD, SKE, and SKEES methods are 13.19%, 13.95%, and 14.0%, respectively, which are all less than the target damping ratio, but still acceptable.

4. SEISMIC RESPONSE OF THE RETROFIT EXAMPLES

Numerical analysis was performed on a 3D model consisting of two structures connected by linear viscous dampers to further verify the control performance of Approaches I and II, as shown in Fig. 10. Structure A represents an existing conventional 8-story hospital structure to be retrofitted. The heights of the first story and the upper stories are 4 m and 3.5 m respectively. The fundamental modal period in the X direction was 0.945 s. Structure B represents three reaction structures (to be newly constructed), each designed with one-by-one spans and each story height identical to the corresponding story in Structure A. Structure B was designed as an 8-story structure for Approach I, but only as a 4-story building for Approach II. The fundamental modal period in the X direction for the 8- story and 4- story versions of Structure B were calculated to be 0.183 s and 0.087 s, respectively. Both structures were assumed to have an inherent damping ratio of 5%.

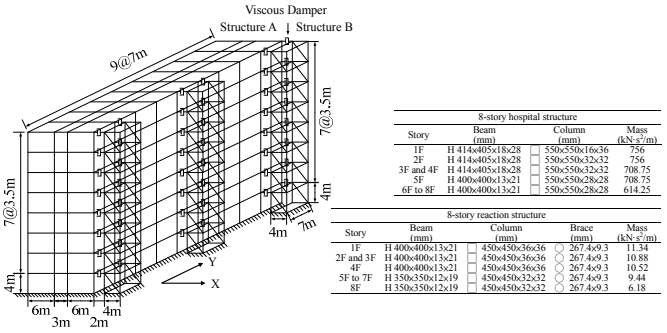

8-story hospital structure

Story	Beam (mm)	Column (mm)	Mass (kN·s²/m)
1F	H 414×405×18×28	550×550×16×36	756
2F	H 414×405×18×28	550×550×32×32	756
3F and 4F	H 414×405×18×28	550×550×32×32	708.75
5F	H 400×400×13×21	550×550×28×28	708.75
6F to 8F	H 400×400×13×21	550×550×28×28	614.25

8-story reaction structure

Story	Beam (mm)	Column (mm)	Brace (mm)	Mass (kN·s²/m)
1F	H 400×400×13×21	450×450×36×36	267.4×9.3	11.34
2F and 3F	H 400×400×13×21	450×450×36×36	267.4×9.3	10.88
4F	H 400×400×13×21	450×450×36×36	267.4×9.3	10.52
5F to 7F	H 350×350×12×19	450×450×32×32	267.4×9.3	9.44
8F	H 350×350×12×19	450×450×32×32	267.4×9.3	6.18

(a) Approach I

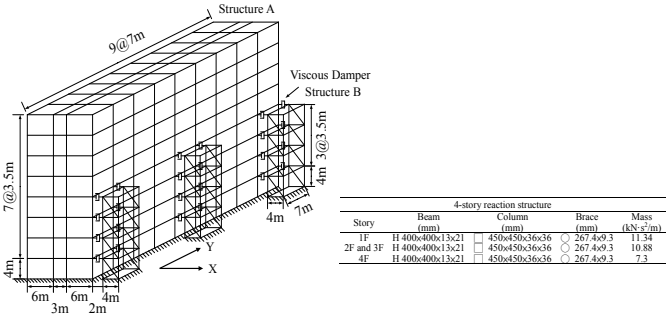

4-story reaction structure

Story	Beam (mm)	Column (mm)	Brace (mm)	Mass (kN·s²/m)
1F	H 400x400x13x21	450x450x36x36	◇ 267.4x9.3	11.34
2F and 3F	H 400x400x13x21	450x450x36x36	◇ 267.4x9.3	10.88
4F	H 400x400x13x21	450x450x36x36	◇ 267.4x9.3	7.3

(b) Approach II

Fig. 10 Retrofit examples of the three-dimensional models.

Based on the reasonable assumption that Structures A and B can be represented by two SDOF systems and a target damping ratio of 15% being set for Structure A, the ω_b/ω_a for Approaches I and II were 5.18 and 10.81, respectively, the c_d/c_b were 8.64 and 7.37, respectively, and the c_d/c_a were the same, i.e., equal to two. If these design parameters were plotted as shown in Fig. 8, it can be shown that they do not fall within an undesired frequency ratio range. The damping coefficients of the different stories of the hospital structure under Approaches I and II are summarized in Table 2. The same trend as in Table 1 is evident.

Table 2 Distributions of the damping coefficients of the 8-story hospital structure for Approaches I and II based on UD, SKE, and SKEES.

Story	Approach I			Approach II		
	UD (kN·s/m)	SKE (kN·s/m)	SKEES (kN·s/m)	UD (kN·s/m)	SKE (kN·s/m)	SKEES (kN·s/m)
8	854.3	1156.7	1222.6	-	-	-
7	854.3	1002.1	1059.2	-	-	-
6	854.3	797.3	842.7	-	-	-
5	854.3	653.9	691.1	-	-	-
4	854.3	408.6	-	5709.0	7582.4	7826.9
3	854.3	215.0	-	5709.0	3989.3	4117.9
2	854.3	84.6	-	5709.0	1570.0	-
1	854.3	13.2	-	5709.0	244.4	-
Total	6834.4	4331.3	3815.5	22836.0	13386.1	11944.8

Two ground motions were used for the subsequent tests. One was the original 1940 El Centro N-S earthquake with an intensity of 0.348 g and the other was a scaled version of the 1999 Chi-Chi earthquake in Taiwan with an intensity of 0.304 g, respectively denoted as El Centro and TCU065 hereafter. The elastic maximum relative displacements and maximum story drift angles of the 8-story hospital structure for Approaches I and II based on the UD, SKE, and SKEES methods are showed in Figs. 11 and 12, respectively.

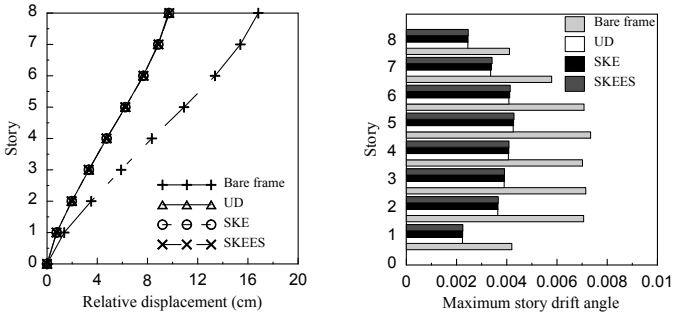

(a) El Centro

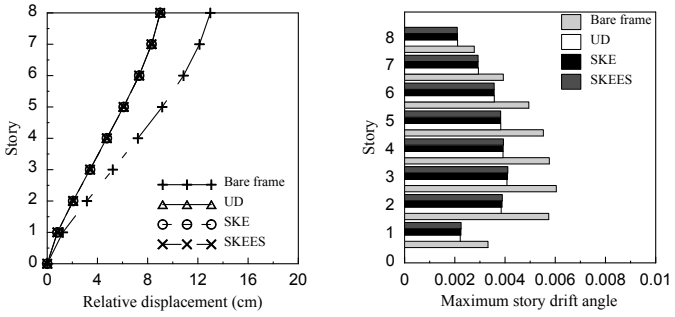

(b) TCU065

Fig. 11 Elastic seismic responses of the 8-story hospital structure for Approach I based on UD, SKE, and SKEES.

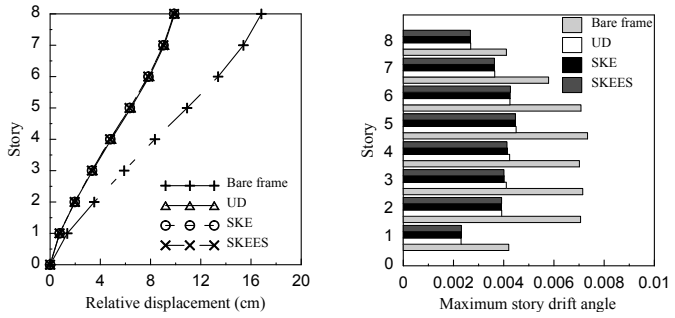

(a) El Centro

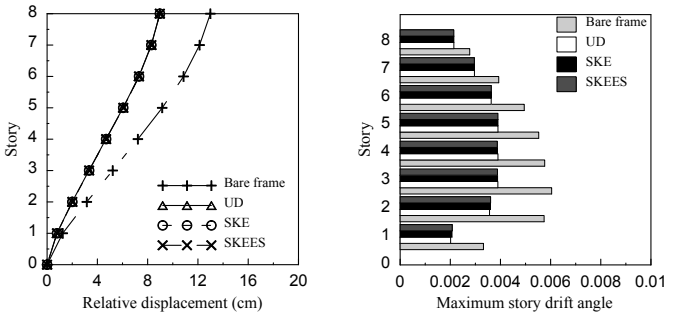

(b) TCU065

Fig. 12 Elastic seismic responses of the 8-story hospital structure for Approach II based on UD, SKE, and SKEES.

From Figs. 11 and 12, it can be seen that whether using Approach I or II and using the UD, SKE or SKEES method, the reconstructed hospital structure exhibits better displacement control performance than the original structure, which means that the external linear viscous damping can effectively reduce the seismic responses of the hospital structure. The relative displacement

and absolute acceleration response histories of the structures are discussed below using the results for Approach I based on the UD, SKE, and SKEES methods subjected to El Centro as showed in Figs. 13 to 15, respectively.

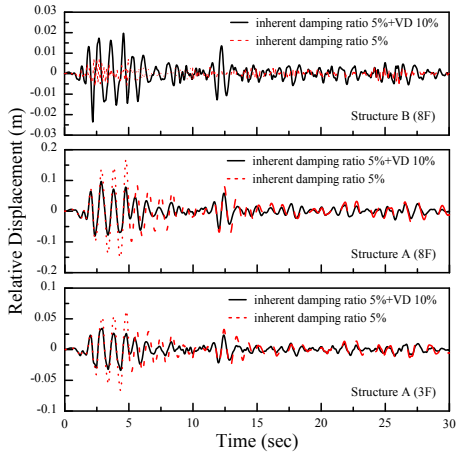

(a) relative displacement response history

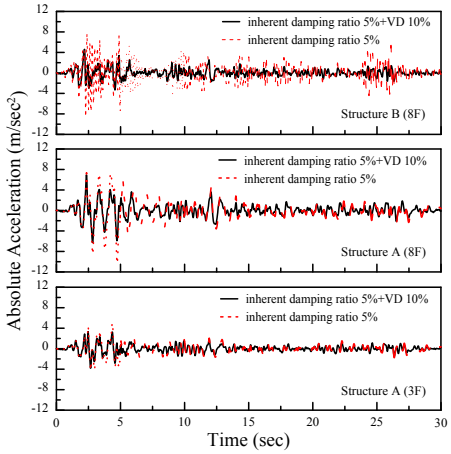

(b) absolute acceleration response history

Fig. 13 Elastic response histories of the 8-story hospital structure and reaction structures for Approach I based on UD under El Centro.

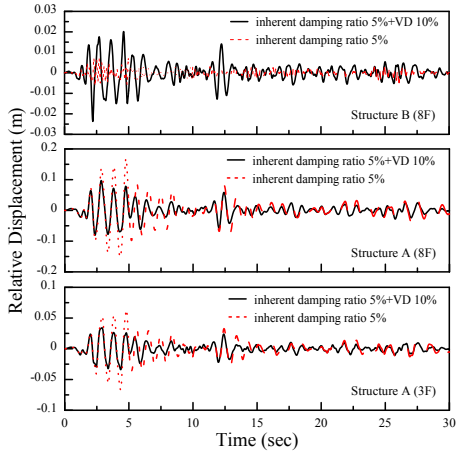

(a) relative displacement response history

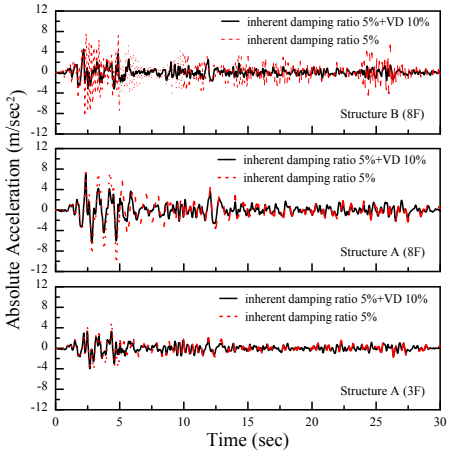

(b) absolute acceleration response history

Fig. 14 Elastic response histories of the 8-story hospital structure and reaction structures for Approach I based on SKE under El Centro.

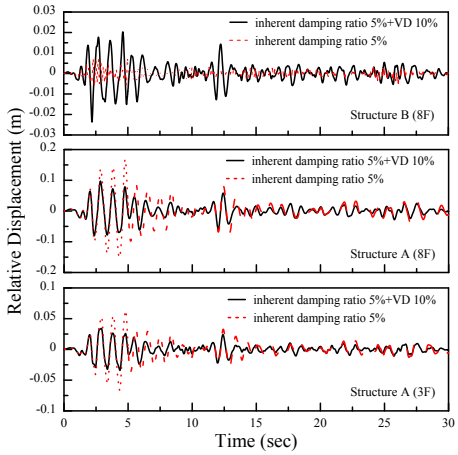

(a) relative displacement response history

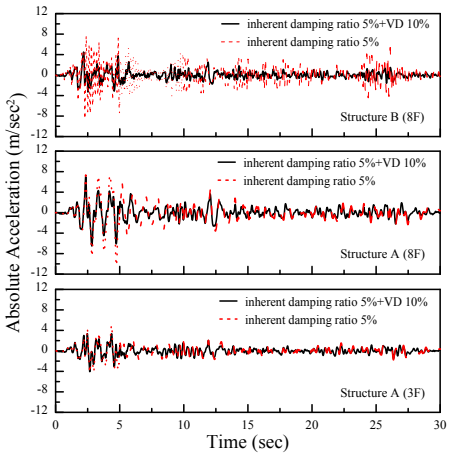

(b) absolute acceleration response history

Fig. 15 Elastic response histories of the 8-story hospital structure and reaction structures for Approach I based on SKEES under El Centro.

These charts clearly show that Approach I was effective in reducing the seismic response of hospital structures, whether using the UD, SKE, or SKEES method. Furthermore, regardless of whether the structures are connected by viscous dampers, the relative displacement responses of the reactive structures are much smaller than those of the unprotected and retrofitted hospital structure. It is worth noting that when the viscous dampers were in place, the displacement responses of the reaction structures were larger than when they were not, which is more realistic than the rigid body assumption in Section 3. Although the effectiveness of linked linear viscous dampers has not been perfectly proven due to the assumptions made when deriving the damping coefficient distribution formula, the results are accurate enough.

A similar procedure was performed for Approach II, but using TCU065. The results for the UD, SKE, and SKEES methods are shown in Figs. 16 to 18. Again, the effectiveness of Approach II in reducing the seismic response of the hospital structure is evident regardless of which method was used.

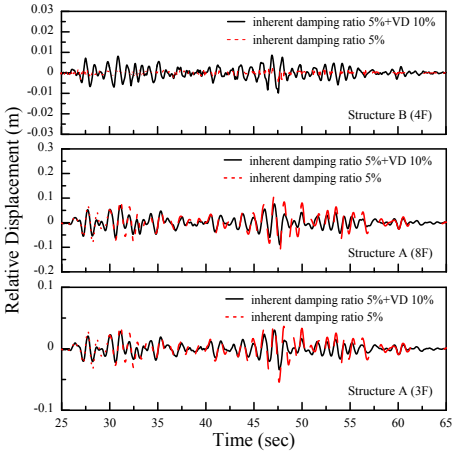

(a) relative displacement response history

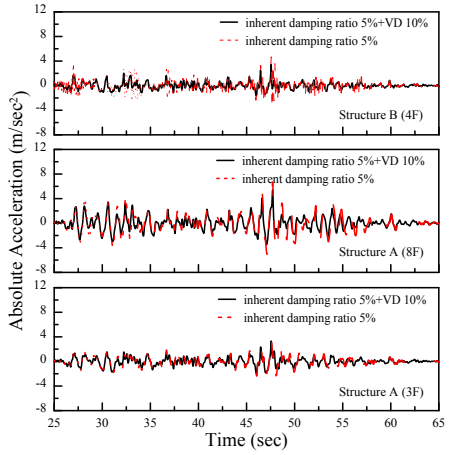

(b) absolute acceleration response history

Fig. 16 Elastic response histories of the 8-story hospital structure and reaction structures for Approach II based on UD under TCU065.

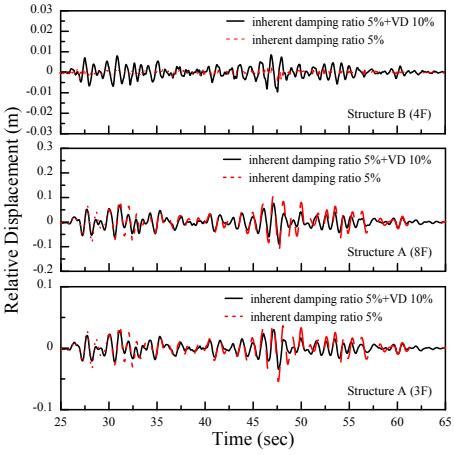

(a) relative displacement response history

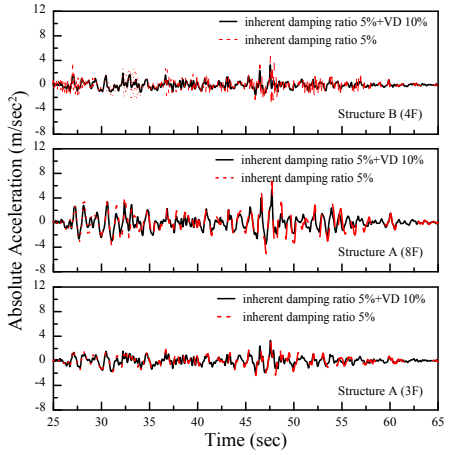

(b) absolute acceleration response history

Fig. 17 Elastic response histories of the 8-story hospital structure and reaction structures for Approach II based on SKE under TCU065.

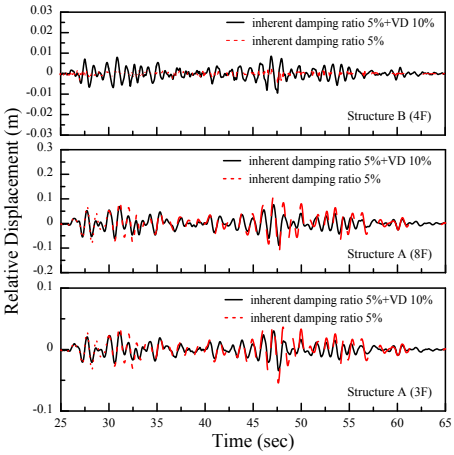

(a) relative displacement response history

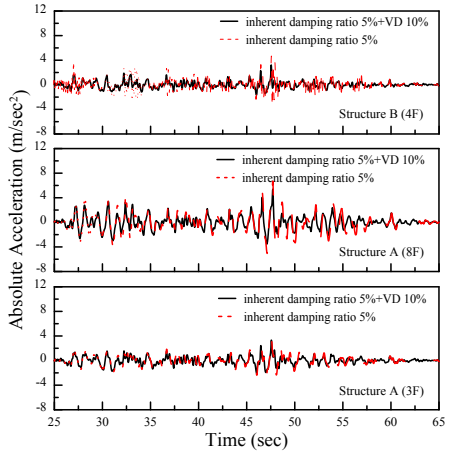

(b) absolute acceleration response history

Fig. 18 Elastic response histories of the 8-story hospital structure and reaction structures for Approach II based on SKEES under TCU065.

The maximum damper forces obtained from the two approaches and the three distribution methods are listed in Table 3. It seems that in all cases, the higher the story to which the viscous damper is attached, the greater the damping force required. With almost the same control performances under El Centro and TCU065, using the UD method always required a larger total damper force than those using the SKE and SKEES methods. It means that using the SKE or SKEES method is more cost-effective than using the UD method for the proposed seismic retrofit strategy. Also, using the SKEES method always required a smaller total damper force than that using the SKE method. Thus, in addition to verifying the conceptual feasibility and effectiveness of distributing the damping coefficients to appropriate stories, using the SKEES method is also significantly more economical than the SKE method. In conclusion, the SKEES approach is a more appealing option for the suggested seismic retrofit plan being more practical and economical than the other two methods.

Table 3 Maximum damper forces at different stories of the 8-story hospital structure for Approaches I and II based on UD, SKE, and SKEES under El Centro and TCU065.

Story	Approach I						Approach II					
	El Centro			TCU065			El Centro			TCU065		
	UD (kN)	SKE (kN)	SKEES (kN)	UD (kN)	SKE (kN)	SKEES (kN)	UD (kN)	SKE (kN)	SKEES (kN)	UD (kN)	SKE (kN)	SKEES (kN)
8	679	903	950	375	511	541	-	-	-	-	-	-
7	624	724	762	344	406	430	-	-	-	-	-	-
6	546	506	533	300	280	297	-	-	-	-	-	-
5	441	339	358	263	202	213	-	-	-	-	-	-
4	338	163	-	219	105	-	2111	2792	2877	1472	1949	2007
3	254	68	-	169	42	-	1474	1077	1122	1097	776	802
2	165	17	-	107	11	-	947	275	-	693	194	-
1	72	1	-	44	1	-	412	19	-	277	12	-
Total	3120	2720	2604	1821	1558	1482	4944	4162	3999	3539	2932	2809

5. CONCLUSIONS

This study developed, analytically evaluated, and numerically examined a seismic retrofit approach for existing hospitals utilizing an external connection via linear viscous dampers whose damping coefficients were distributed in a more efficient manner. The following conclusions were drawn:

- Modal composite damping ratios and phase lag variations with respect to different frequency ratios and damping coefficient ratios are seen from the analysis results of a model consisting of two adjacent single-degree-of-freedom (SDOF) systems linked by linear viscous dampers. For the seismic retrofit proposals, the undesired frequency ratios can be excluded to avoid improper design of the new reaction structures and connected dampers.
- In addition to the uniform distribution (UD), the distributions based on story kinetic energy (SKE) and story kinetic energy to efficient stories (SKEES) were also used to calculate the damping coefficient distribution of the connected linear viscous dampers Under the ground acceleration excitation, a 10-story hospital structure was found to have a damping ratio close to the target value when retrofitted with linear viscous dampers connecting all stories (Approach I) and only a partial connection involving lower stories (Approach II).
- Whether using Approach I or Approach II and using the UD, SKE, or SKEES method, the retrofitted hospital structures had the same target damping ratio under El Centro and TCU065, so they all had comparable control performance. Moreover, they exhibited excellent seismic performance compared to the unprotected hospital structure.
- Under El Centro and TCU065, whether using Approach I or Approach II and using the UD, SKE, or SKEES method, the higher the story connected by viscous dampers, the greater the damping force required. With almost the same control performance, the UD method required a larger total damping force than the SKE and SKEES methods, while the SKEES method required the smallest damping force. Therefore, the SKE method is sufficiently economical if only considering the cost of viscous dampers, while the SKEES method is the overall most cost-effective

method for the proposed seismic retrofit strategy.

- In the examples of this study, only two ground motions were used as seismic inputs and the elastic responses were numerically examined. The generality and applicability of the proposed seismic retrofit strategy may not yet be fully demonstrated. In the future, more seismic scenarios and larger inelastic seismic responses may be considered.

REFERENCES

Alesch, D.J., Arendt, L.A. and Petak, W.J. (2005). "Seismic Safety in California Hospitals: Assessing an Attempt to Accelerate the Replacement or Seismic Retrofit of Older Hospital Facilities." no. NCEER-05-0006, National Center for Earthquake Engineering Research, State University of New York at Buffalo, New York, USA.

Bachman, R.E., Hamburger, R.O., Comartin, C.D., Rojahn, C. and Whittaker, A.S. (2003). "Framework for Performance-Based Design of Nonstructural Components." *Seminar on Seismic Design, Performance and Retrofit of Nonstructural Components in Critical Facilities*, California, USA.

Bhaskararao, A.V. and Jangid, R.S. (2007). "Optimum Viscous Damper for Connecting Ddjacent SDOF Structures for Harmonic and Stationary White-Noise Random Excitations." *Earthq. Eng. Struct. Dyn*. **36**(4) 563-571.

FEMA 273 (1997). *NEHRP Guidelines for the Seismic Rehabilitation of Buildings*. Building Seismic Safety Council for the Federal Emergency Management Agency, Washington, D.C..

FEMA 356 (2000). *Prestandard and Commentary for the Seismic Rehabilitation of Buildings*. American Society of Civil Engineers for the Federal Emergency Management Agency, Washington, D.C..

Hamburger, R.O. (2003). "A Vision of the ATC-58 Project, Developing of Performance-Based Seismic Guidelines." *Programming Workshop on Performance-Based Design*, Applied Technology Council, California, USA.

Hwang, J.S., Huang, Y.N., Yi, S.L. and Ho, S.Y. (2008). "Design Formulations for Supplemental Viscous Dampers to Building Structures." *J. Struct. Eng*. **134**(1) 22-31.

Hwang, J.S., Lin, W.C. and Wu, N.J. (2013). "Comparison of Distribution Methods for Viscous Damping Coefficients to Buildings." *Struct. Infrastruct. Eng*. **9**(1) 28-41.

Hwang, J.S., Wang, S.J., Huang, Y.N. and Chen, J.F. (2007). "A seismic Retrofit Method by Connecting Viscous Dampers for Microelectronics Factories." *Earthq. Eng. Struct. Dyn*. **36**(11) 1461-1480.

Lin, T.K., Hwang, J.S. and Chen, K.H. (2017). "Optimal Distribution of Damping Coefficients for Viscous Dampers in Buildings." *Int. J. Struct. Stab. Dyn*. **17**(4) 1750054.

Maison, B.F. and Kasai, K. (1992). "Dynamics of Pounding When Two Buildings Collide." *Earthq. Eng. Struct. Dyn*. **21**(9) 771-786.

Matsagar V.A. and Jangid R.S. (2005). "Viscoelastic Damper Connected to Adjacent Structures Involving Seismic Isolation." *J. Civ. Eng. Manag*. **11**(4) 309-322.

Nagarajaiah, S. and Xiaohong, S. (2000). "Response of Base-Isolated USC Hospital Building in Northridge Earthquake." *J. Struct. Eng*. **126**(10) 1177-1186.

Seleemah, A.A. and Constantinou, M.C. (1997). "Investigation of Seismic Response of Buildings with Linear and Nonlinear Fluid Viscous Dampers." no. NCEER-97-0004, National Center for Earthquake Engineering Research, State University of New York at Buffalo, New York, USA.

Singh, M.P. and Moreschi, L.M. (2002). "Optimal Placement of Dampers for Passive Response Control." *Earthq. Eng. Struct. Dyn*. **31**(4) 955-976.

Takewaki, I. (2005). "Optimal Damper Placement for Minimum Transfer Functions." *Earthq. Eng. Struct. Dyn*. **26**(11) 1113-1124.

Wongprasert, N. and Symans, M.D. (2004). "Application of A Genetic Algorithm for Optimal Damper Distribution within the Nonlinear Seismic Benchmark Building." *J Eng Mech*. **130**(4) 401-406.

Xu, Y.L., He, Q. and Ko, J.M. (1999). "Dynamic w of Damper-Connected Adjacent Buildings under Earthquake Excitation." *Eng. Struct*. **21**(2) 135-148.

Zhang, W.S. and Xu, Y.L. (1999). "Dynamic Characteristics and Seismic Response of adjacent Buildings Linked by Discrete Dampers." *Earthq*. *Eng. Struct. Dyn*. **28**(10) 1163-1185.

Zhang, W.S. and Xu, Y.L. (2000). "Vibration Analysis of Two Buildings Linked by Maxwell Model-Defined Fluid Dampers." *J. Sound Vib*. **233**(5) 775-796.